Electronic Supplementary Material (ESI) for Chemical Communications
This journal is © The Royal Society of Chemistry 2022

Electronic supplementary information

Effective taste masking of alkaloids by a water-soluble terphen[3]arene

Junyi Chen,[ab] Longming Chen,[b] Yahan Zhang,[b] Liang Zhao,[b] Ming Dong,[a] Zhao Meng,[b] Qingbin Meng,*[b] and Chunju Li*[a]

[a] Key Laboratory of Inorganic-Organic Hybrid Functional Material Chemistry, Ministry of Education, Tianjin Key Laboratory of Structure and Performance for Functional Molecules, College of Chemistry, Tianjin Normal University, Tianjin 300387, P. R. China.

[b] State Key Laboratory of Toxicology and Medical Countermeasures, Beijing Institute of Pharmacology and Toxicology, Beijing 100850, P. R. China.

Table of Contents

1. General materials and methods

1.1 Materials. All reagents were purchased commercially and used without further purification unless otherwise noted. Palmatine was purchased from Innochem Technology Co. Ltd. (Beijing, China). Berberine, colchicine and arecoline were obtained from Senrise Technology Co. Ltd. (Anhui, China). Atropinol was purchased from Alta Scientific Co. Ltd. (Tianjin, China). Thephylline was purchased from Bide Pharmatech Co. Ltd. (Shanghai, China). Acridine Orange (AO) was obtained from Alfa Aesar Chemical Co. Ltd. (Shanghai, China).

1.2 Instruments. ^{1}H NMR data was measured by JNM-ECA-400 spectrometer, JEOL Ltd. Fluorescence spectroscopic studies were carried out by a LS-55 fluorescence spectrophotometer, PerkinElmer, Inc. Bitterness scores were determined by TS-5000Z taste sensing system, INSENT. Cytotoxicity studies were performed on SpectraMax ® M5 plate reader, Molecular Devices.

1.3 Cell, animals and bacterial strains. Human gastric mucosal epithelial cells (GES-1) were cultured in DMEM supplemented with 10% FBS, 1% penicillin and 1% streptomycin. Then cells were incubated at 37 ^{o}C under 5% CO_2 and 90% relative humidity, and passaged every 2 days.

Six-week-old Balb/c mice (~20 g body weight) of both sexes were purchased from SPF Biotechnology Co. Ltd. (Beijing, China) and maintained at 25 °C in a 12 h light/dark cycle with free access to food and water. Animals were allowed to acclimate to environment for at least one week before experiments. All experimental procedures were conducted in accordance with the Guide for the Care and Use of Laboratory Animals of the AAALAC, and were approved by the Animal Care and Use Committee of the National Beijing Center for Drug Safety Evaluation and Research. Best efforts were made to minimize the number of animals used and their suffering.

The bacterial strains used in this study included Gram-postive *S .aureus* (ATCC 25922) and Gram-negative *E .coli* (ATCC 25922). All strains were maintained in 80 % sterile glycerol at -80 ^{o}C. After being thawed, the aliquots were diluted (1 : 2000) in fresh sterile broth and grown overnight at 37 ^{o}C with agitation.

1.4 Fluorescence titration.[1] To quantitatively investigate the complexation behavior between STP3 and alkaloids, fluorescence competitive titration was respectively performed in PBS buffer (10 mM, pH = 6.8) and HCl solution (pH = 1.2) by equation 1. We considered that a guest formed a 1:1 host:guest complex with a host at an association constant (K_a), which satisfied the respective law of mass action relating to the equilibrium concentrations of free host ([H]), free guest ([G]) and host-guest complex ([HG]). The relationship between the total concentration of host ($[H]_0$), guest ($[G]_0$) and their equilibrium concentrations were introduced by the law of mass conservation (equation 2-1 and 2-2). Here $[G]_0$ was the initial concentration of guest as a known parameter, which was kept constant in the titration process. Then equation 1 and 2-2 were employed to deduced equation 3. When the fluorescence titration was performed, the intensity of fluorescence (F) corresponded to the combined intensity of the host and the host-guest complex, which were described by molar fractions (equation 4). Both F_{HG} and F_G were known parameters in which F_G was the fluorescent of $[G]_0$ and F_{HG} was the fluorescent intensity when all guests were complexed. The equation 5 deduced by equation 2-1, 2-2, 3 and 4, explained the relationship between K_a and variables $[H]_0$ in fluorescence titration.

$$[\mathrm{H}] + [\mathrm{G}] \overset{K_a}{\leftrightarrow} [\mathrm{HG}]$$

$$K_a = \frac{[\mathrm{HG}]}{[\mathrm{H}][\mathrm{G}]} \quad (1)$$

$$[\mathrm{G}] = [\mathrm{G}]_0 - [\mathrm{HG}] \quad (2\text{-}1)$$

$$[\mathrm{H}] = [\mathrm{H}]_0 - [\mathrm{HG}] \quad (2\text{-}2)$$

$$[\mathrm{HG}] = \frac{K_a[\mathrm{H}][\mathrm{G}]_0}{1 + K_a[\mathrm{H}]} \quad (3)$$

$$F = \frac{[\mathrm{HG}]}{[\mathrm{G}]_0} F_{\mathrm{HG}} + \frac{[\mathrm{G}]}{[\mathrm{G}]_0} F_{\mathrm{G}} \quad (4)$$

$$F = F_{\mathrm{HG}} + (F_{\mathrm{G}} - F_{\mathrm{HG}}) \frac{\left([\mathrm{G}]_0 - [\mathrm{H}]_0 - \frac{1}{K_a}\right) - \sqrt{([\mathrm{G}]_0 - [\mathrm{H}]_0 - \frac{1}{K_a})^2 + 4[\mathrm{H}]_0[\mathrm{G}]_0}}{2[\mathrm{G}]_0} \quad (5)$$

To proceed the competitive titrations, we considered competitors that could competitively bind to host in a 1:1 stoichimetry at an association constant (Kc, equation 6). Free host (H), free competitor (C) and host-competitor complex (HC) obeyed the respective law of mass action referring to equilibrium concentrations. Here the total

concentration of host ($[H]_0$), competitor ($[C]_0$) and their equilibrium concentrations satisfied the law of mass conservation (equation 7). In the course of titration, the fluorescence intensity (F_C) was expressed as a linear combination of F_{HG} and F_G, weighted by their molar fractions on the basis of equation 8. Through a 1:1 host-guest binding model, F_{HG} was the initial experimental fluorescence intensity in the absence of C. Substituting equation 3 into equation 8 gave equation 9, with the concentration of uncomplexed host as an unknown parameter ([H]), which was numerically solved by equation 10. Note: equation 10 was deduced by combination equation 3, 6, 7-1 and 7-2. For fitting, the fluorescence intensity was plotted against $[C]_0$ based on equation 9.

$$[H] + [C] \overset{K_C}{\leftrightarrow} [HC]$$

$$K_C = \frac{[HC]}{[H][C]} \quad (6)$$

$$[H] = [H]_0 - [HG] - [HC] \quad (7\text{-}1)$$

$$[C] = [C]_0 - [HC] \quad (7\text{-}2)$$

$$F_C = \frac{[HG]}{[G]_0} F_{HG} + \frac{[G]}{[G]_0} F_G \quad (8)$$

$$F_C = F_G + (F_{HG} - F_G) \frac{K_a[H]}{1 + K_a[H]} \quad (9)$$

$$0 = A[H]^3 + B[H]^2 + C[H] + D$$
$$A = K_a K_C$$
$$B = K_a + K_C + K_a K_C([G]_0 + [C]_0 - [H]_0)$$
$$C = K_C([C]_0 - [H]_0) - K_a([H]_0 - [G]_0) + 1$$
$$D = -[H]_0 \quad (10)$$

1.5 Evaluation of taste masking efficiency by electronic tongue. Accurate weighing above alkaloids to prepare 50 μM sample liquid (100 mL). After activation, calibration and diagnosis, evaluation of taste masking efficiency by electronic tongue was carried out at room temperature. Data collection time was 120 s and repeated three times in parallel. Analyzing and converting membrane potential to afford response values indicated degree of bitter taste.

The solution used:

Reference: Tartaric acid solution containing potassium chloride.

Negative electrode: mixture solution of hydrochloride acid, ethanol and deionized water.

Positive electrode: acetonitrile and deionized water containing potassium chloride and potassium hydroxide.

1.6 Biosafety evaluation of STP3. The relative cytotoxicity of STP3 against GES-1 cells was assessed *in vitro* by CCK-8 according to the manufacture's instruction. STP3 was dissolved in PBS and diluted to the required concentration and then added to well-cultured cells to further incubate for 24 h. Subsequently, 10 μL of CCK-8 was added and incubated for 0.5 h. The plate was then recorded on a plate reader. Cell viability was calculated using the method reported previously.[2] In addition, after two-bottle preference test, body weights of mice were recorded at predetermined intervals (on days 0, 2, 4, 6, 8, 10, 12 and 14). For histological analysis of stomach, intestine and major organs (heart, liver, spleen, lung and kidney) were collected after two-bottle preference test, and fixed in 4 % paraformaldehyde. Then paraffin embedded sections were conducted for hematoxylin and eosin (H&E) staining, and examined by a digital scanning system.

1.7 Two-bottle preference test. Before two-bottle preference test, the mice were housed with two bottles of distilled water for being accustomed to have two tips to drink water. After that, 30 mice were randomly divided into three groups. Mice were respectively treated with one bottle containing distilled water and another one containing STP3 (50 μM), palmatine (50 μM) or palmatine/STP3 (50/50 μM). Two bottles have paralleled position with the same angle of tip. Each solution was tested for 48 h. To avoid the side preference caused by the unaltered position, the positions of two bottles were switched after 24 h of each 48-hour test.[3]

1.8 Antibacterial experiments. The antibacterial activities of STP3, palmatine and palmatine/STP3 were determined in sterile 96-well plates by the broth microdilution method. The thawy bacterial strains were incubated with shaking at 180 rpm in 5 mL of the sterile broth at 37 °C. After overnight incubation, the concentration of bacteria reached 1×10^9 CFU·mL^{-1}. Then bacterial suspensions were diluted (1:2000, approximately 2×10^5 CFU·mL^{-1}) and incubated with different concentration of samples in sterile 96-well plates at 37 °C for 24 h with continuous shaking. The minimal inhibitory concentration (MIC) was determined by visual observation combined with absorbance measurement at 600 nm with a plate reader.[4]

2. Synthesis of STP3

TP3-OMe was synthesized and purified according to the procedure reported previously.[5]

Synthesis of TP3-OH

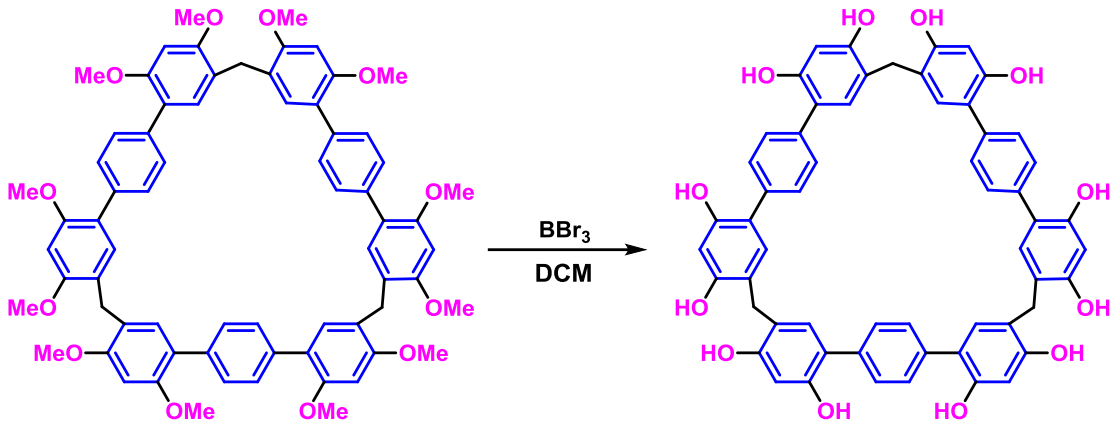

TP3-OMe **TP3-OH**

To a solution of TP3-OMe (1.00 g, 0.92 mmol) in dichloromethane (50 mL), boron tribromide (5.53 g, 22.08 mmol) was added under nitrogen atmosphere and the reaction was stirred at room temperature for 2 days. The mixture was poured into ice water and the precipitate was filtered. Then, the precipitate was washed with ice water and dried to afford a brown solid TP3-OH (0.78 g, 0.85 mmol, yield: 92%). ^{1}H NMR (400 MHz, $(CD_3)_2CO$) δ (ppm): 8.60 (s, 6H), 8.00 (s, 6H), 7.48 (s, 12H), 7.16 (s, 6H), 6.55 (s, 6H), 3.89 (s, 6H). ^{13}C NMR (100 MHz, $(CD_3)_2CO$) δ (ppm): 155.02, 154.12, 137.45, 132.80, 129.52, 121.41, 120.22, 104.00, 23.31. HR-MS (ESI): $C_{57}H_{42}O_{12}NH_4^+$, calcd *m/z* 936.3015; found *m/z* 936.3029.

Synthesis of STP3

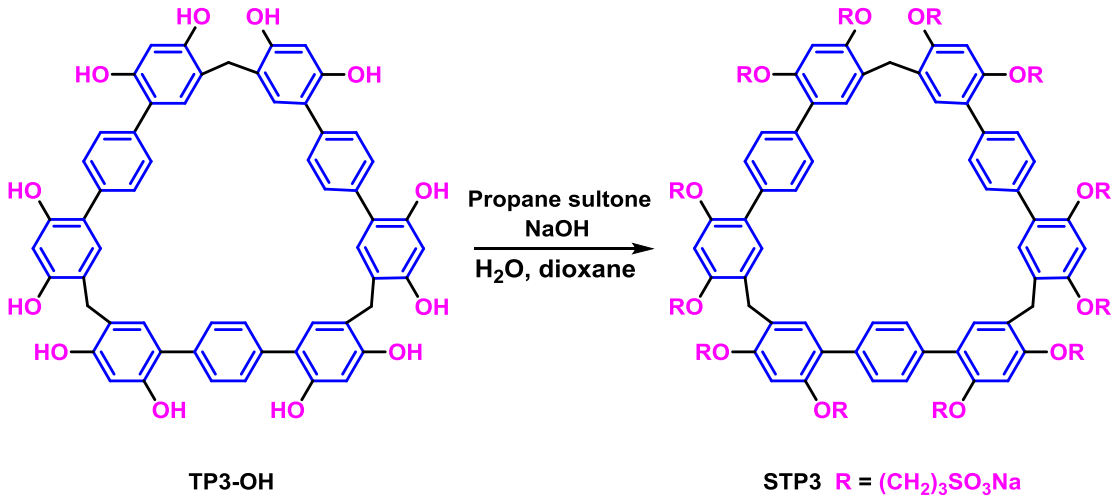

Under nitrogen atmosphere TP3-OH (0.200 g, 0.218 mmol) was dissolved in 10% aqueous sodium hydroxide (5 mL) and treated dropwise with a solution of propane solution (0.479 g, 3.924 mmol) in 1,4-dioxane (5 mL). This solution was stirred at 90 ^{o}C for 5 days. After removal of solvent, the crude solid was redissolved in deionized water (10 mL) and purified by reverse-phase high-performance liquid chromatography (HPLC) using a C8 column (Waters, USA) and a gradient of acetonitrile and deionized water containing 0.1% TFA. The solvent evaporated via lyophilization process to get a brown solid STP3 (0.138 g, 0.052 mmol, yield: 24%). ^{1}H NMR (400 MHz, $(CD_3)_2SO$) δ (ppm): 7.38 (br, 12H), 6.73 (br, 6H), 6.56 (br, 6H), 4.13 (br, 24H), 6.16 (s, 6H), 2.67 (br, 24H), 2.03 (br, 24H). ^{13}C NMR (100 MHz, $(CD_3)_2SO$) δ (ppm): 156.49, 154.56, 153.41, 136.15, 128.55, 121.07, 120.03, 119.16, 100.43, 98.09, 67.20, 48.14, 25.30.

3. Supporting results and experimental raw data

3.1 Characterization of synthetic molecular host.

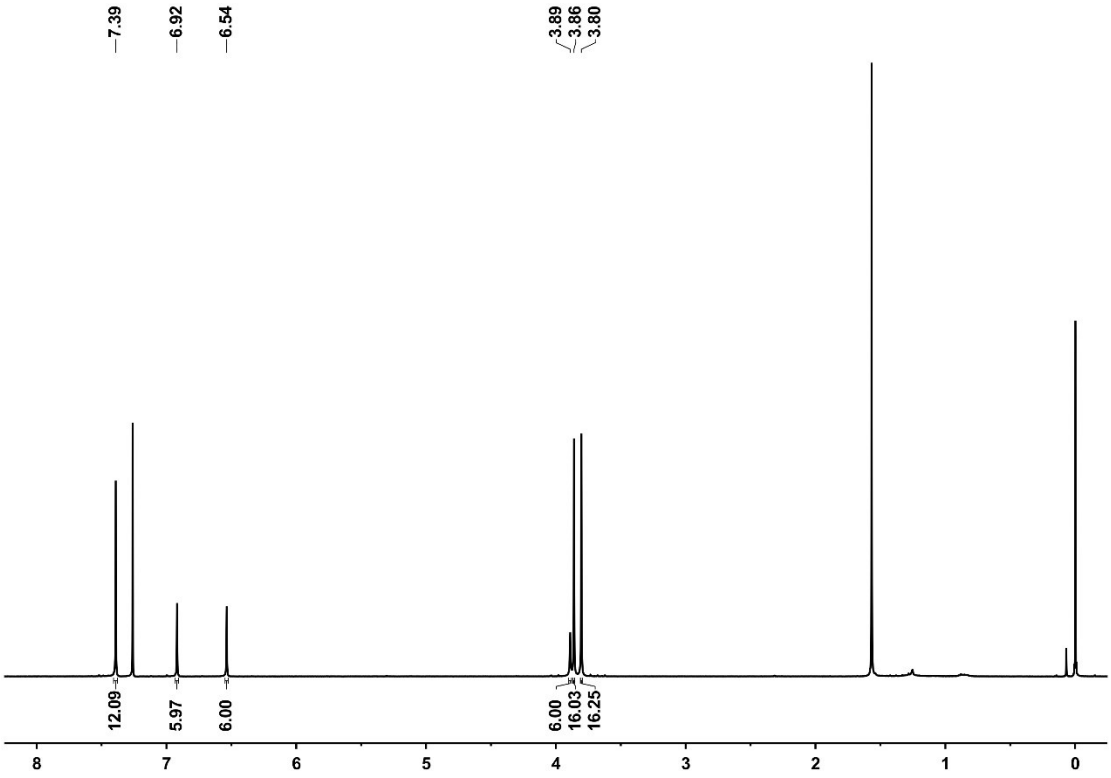

Fig. S1. ^{1}H NMR spectrum (400 MHz, $CDCl_3$) of TP3-OMe.

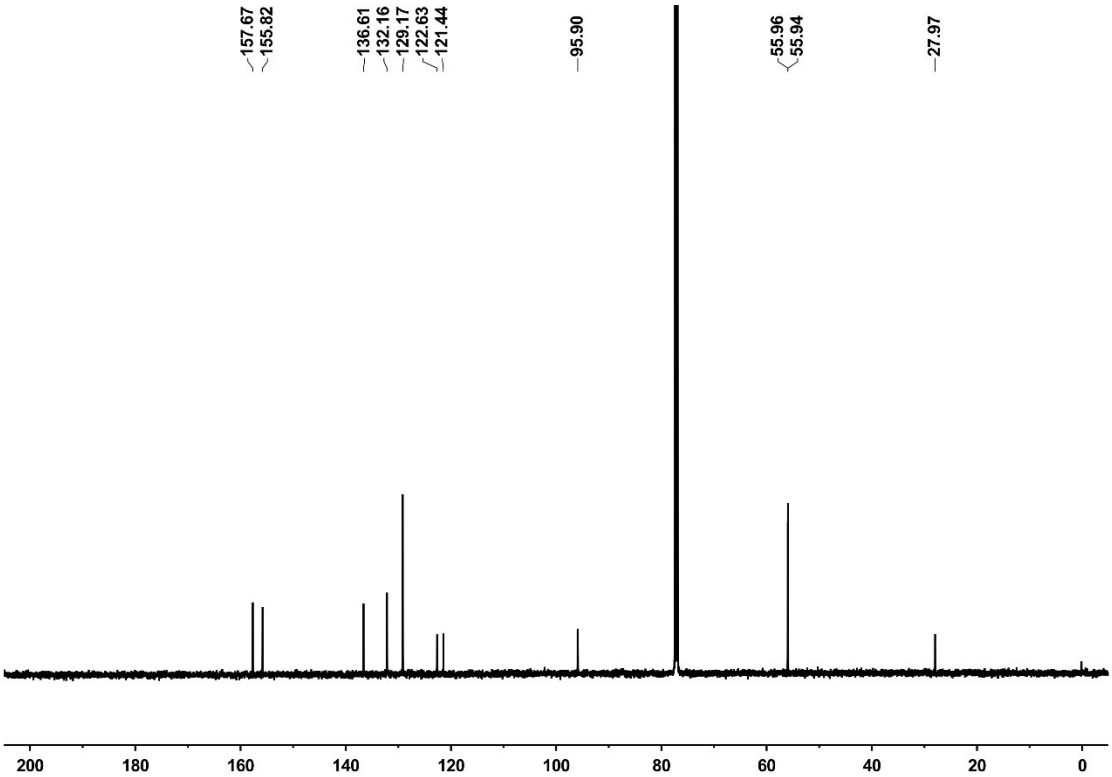

Fig. S2. ^{13}C NMR spectrum (100 MHz, $CDCl_3$) of TP3-OMe.

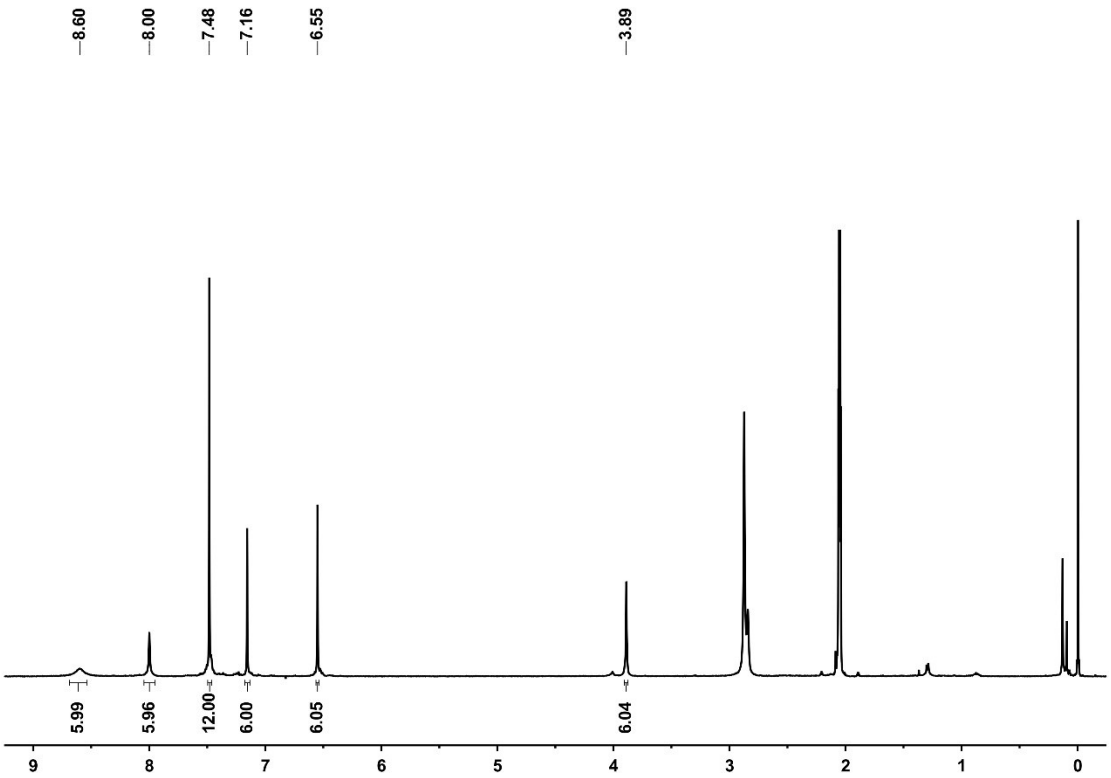

Fig. S3. ^{1}H NMR spectrum (400 MHz, $(CD_3)_2CO$) of TP3-OH.

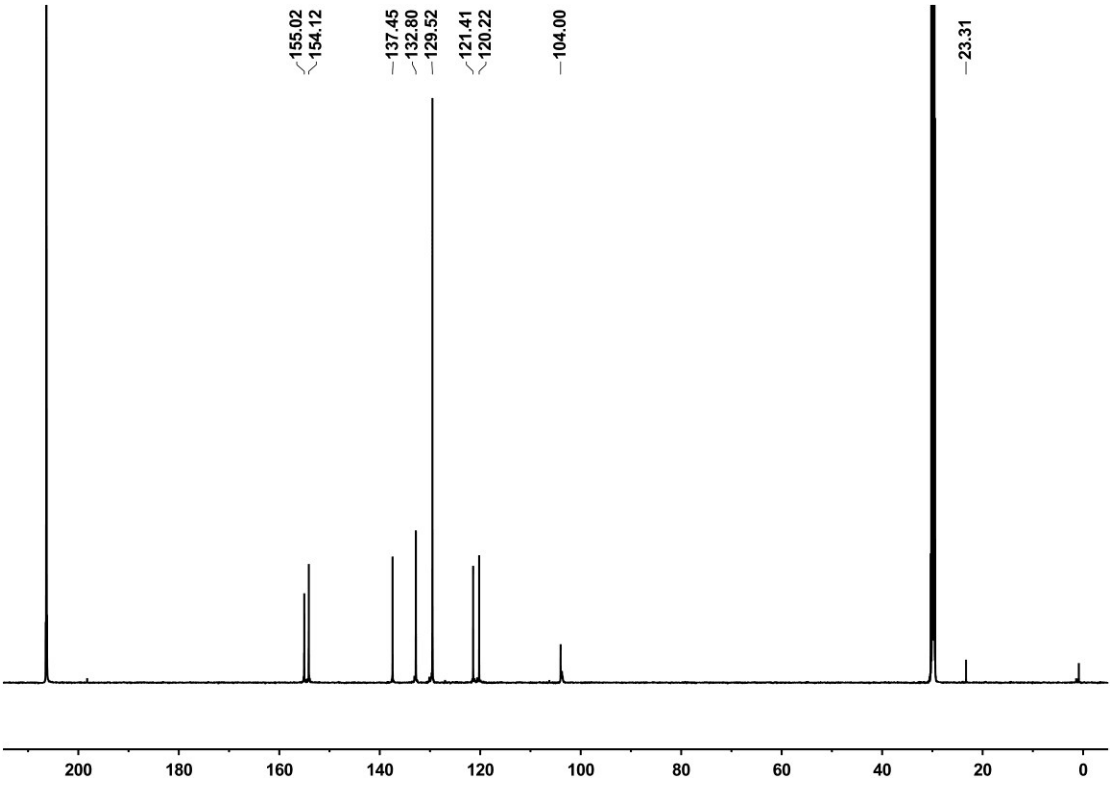

Fig. S4. ^{13}C NMR spectrum (100 MHz, $(CD_3)_2CO$) of TP3-OH.

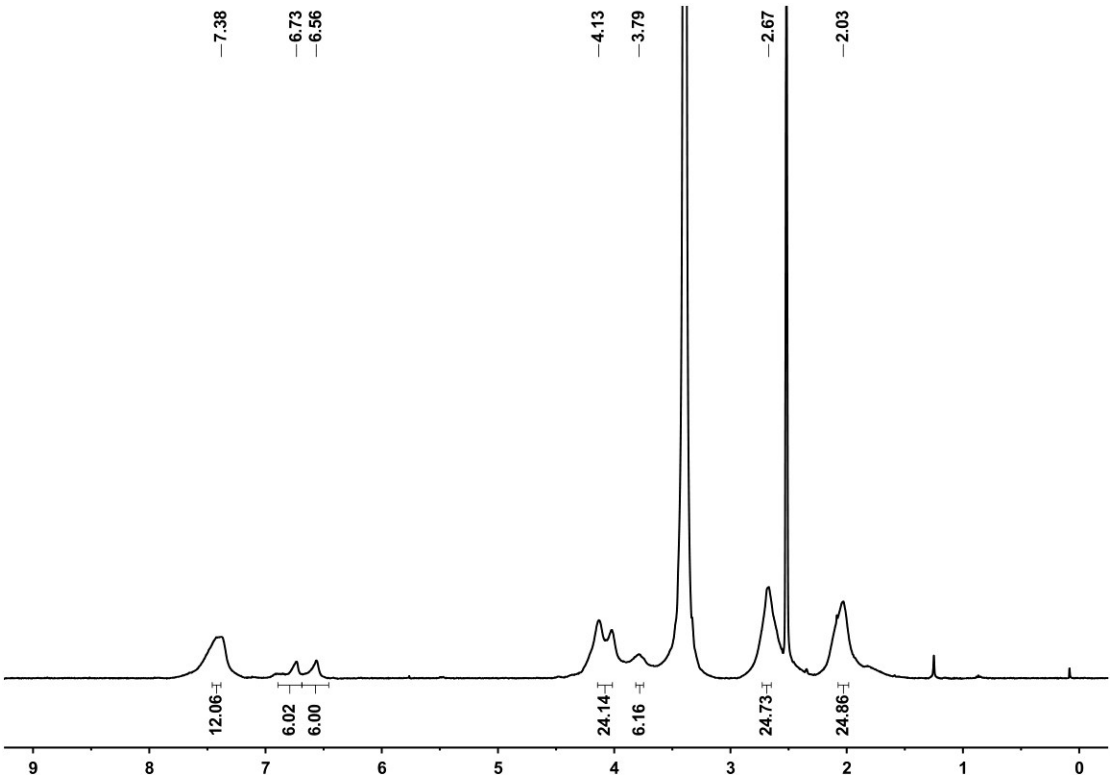

Fig. S5. ^{1}H NMR spectrum (400 MHz, $(CD_3)_2SO$) of STP3.

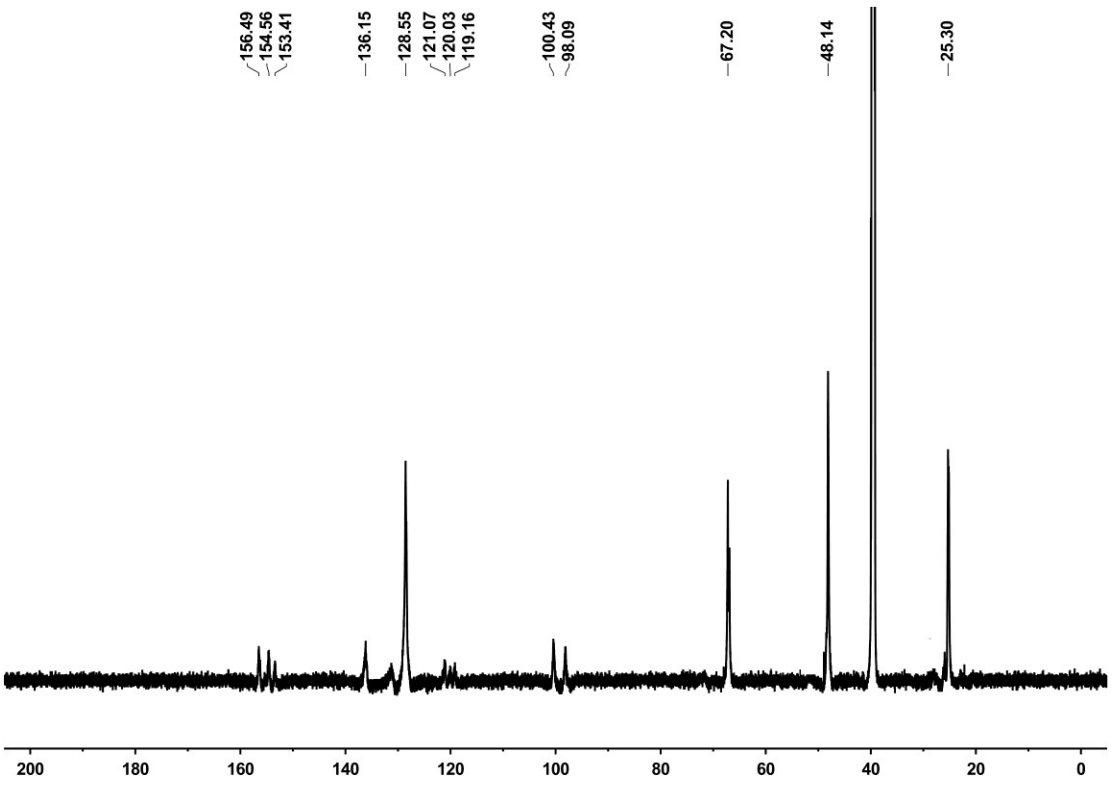

Fig. S6. ^{13}C NMR spectrum (100 MHz, $(CD_3)_2SO$) of STP3.

3.2 Job's plot analysis for complexation of AO with STP3.

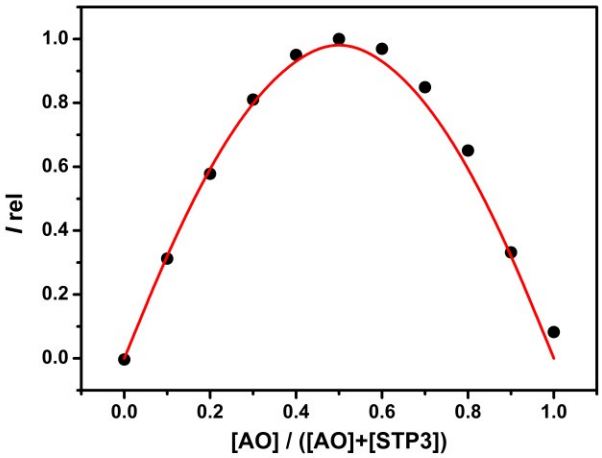

Fig. S7. Job's plot for STP3 with AO in 10 mM PBS buffer at pH 6.8 (λ_{ex} = 492 nm, λ_{em} = 523 nm, [STP3] + [AO] = 1.0 μM).

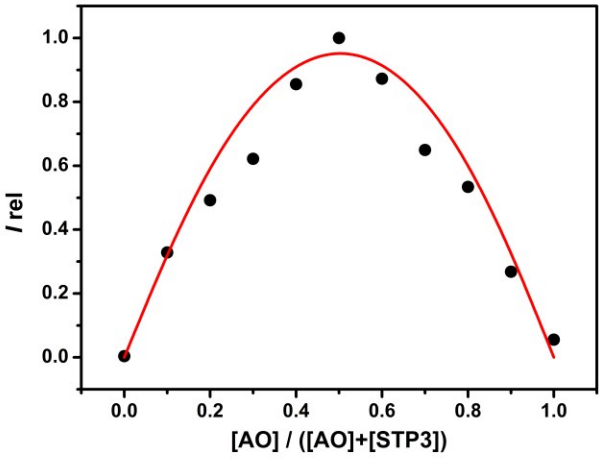

Fig. S8. Job's plot for STP3 with AO in HCl solution at pH 1.2 (λ_{ex} = 492 nm, λ_{em} = 523 nm, [STP3] + [AO] = 1.0 μM).

3.3 Binding affinities between STP3 and alkaloids.

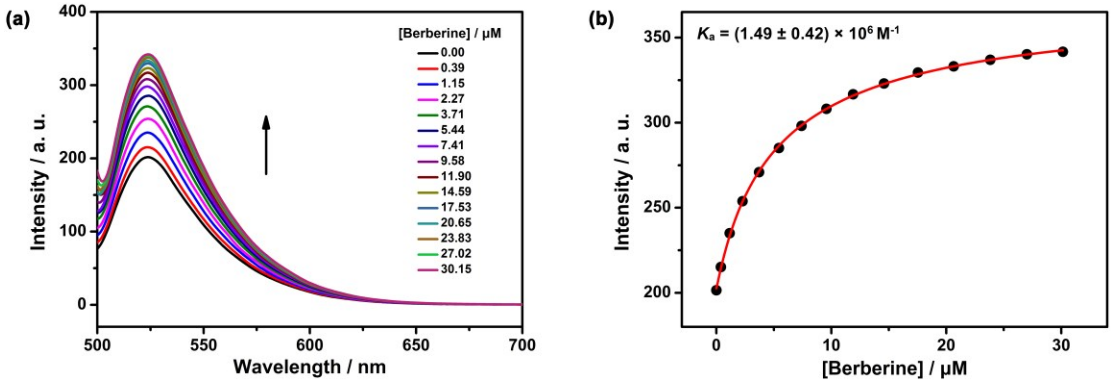

Fig. S9. (a) Competitive fluorescence titration of berberine in the presence of AO/STP3 (1.0/1.0 μM) in PBS buffer (10 mM, pH = 6.8), λ_{ex} = 492 nm. (b) The associated titration curve at λ_{em} = 523 nm and fit according a 1:1 competitive binding model. Data are from n =3 independent experiments and are presented as mean ± SD.

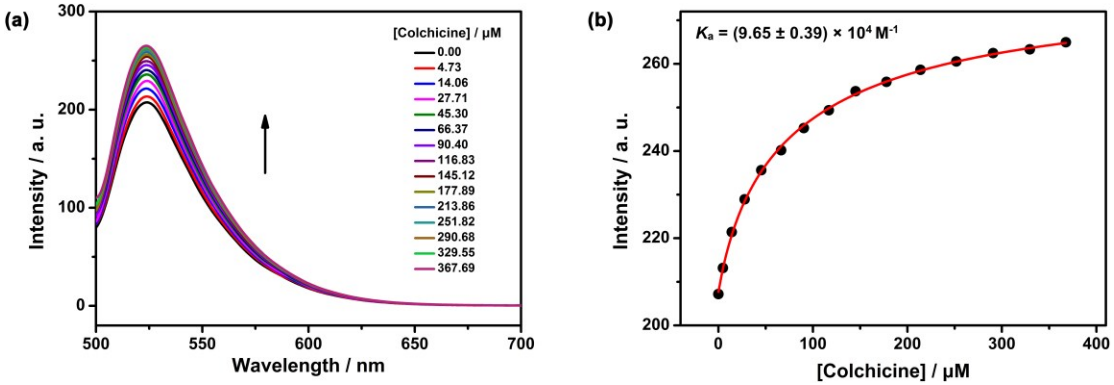

Fig. S10. (a) Competitive fluorescence titration of colchicine in the presence of AO/STP3 (1.0/1.0 μM) in PBS buffer (10 mM, pH = 6.8), λ_{ex} = 492 nm. (b) The associated titration curve at λ_{em} = 523 nm and fit according a 1:1 competitive binding model. Data are from n =3 independent experiments and are presented as mean ± SD.

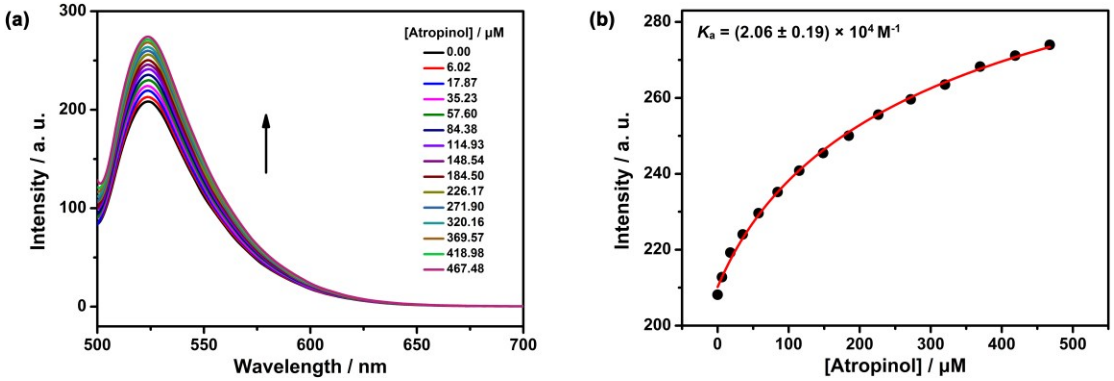

Fig. S11. (a) Competitive fluorescence titration of atropinol in the presence of AO/STP3 (1.0/1.0 μM) in PBS buffer (10 mM, pH = 6.8), λ_{ex} = 492 nm. (b) The associated titration curve at λ_{em} = 523 nm and fit according a 1:1 competitive binding model. Data are from n =3 independent experiments and are presented as mean ± SD.

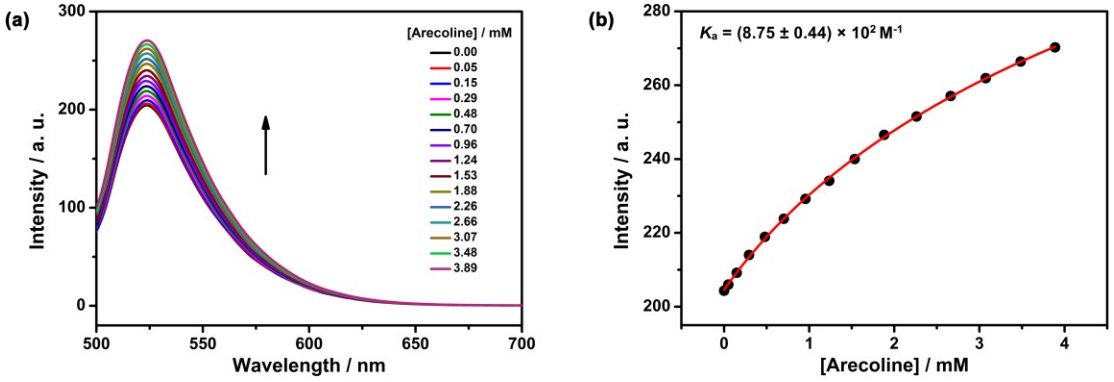

Fig. S12. (a) Competitive fluorescence titration of arecoline in the presence of AO/STP3 (1.0/1.0 μM) in PBS buffer (10 mM, pH = 6.8), λ_{ex} = 492 nm. (b) The associated titration curve at λ_{em} = 523 nm and fit according a 1:1 competitive binding model. Data are from n =3 independent experiments and are presented as mean ± SD.

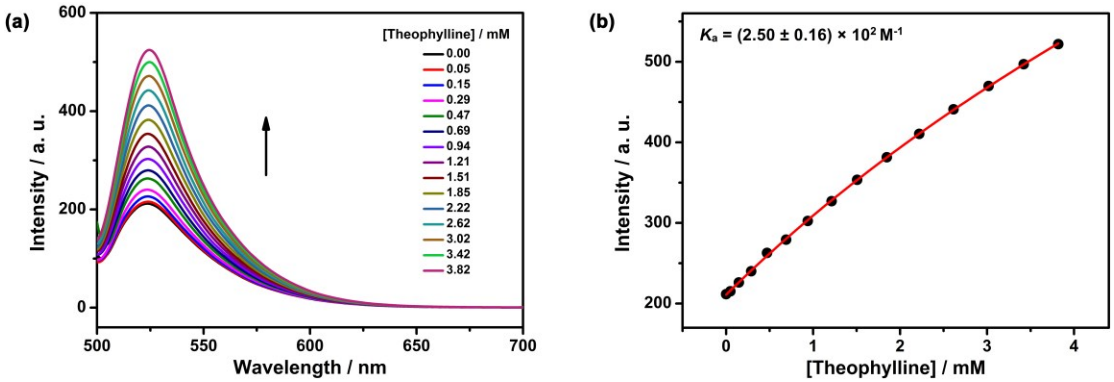

Fig. S13. (a) Competitive fluorescence titration of theophylline in the presence of AO/STP3 (1.0/1.0 μM) in PBS buffer (10 mM, pH = 6.8), λ_{ex} = 492 nm. (b) The associated titration curve at λ_{em} = 523 nm and fit according a 1:1 competitive binding model. Data are from n =3 independent experiments and are presented as mean ± SD.

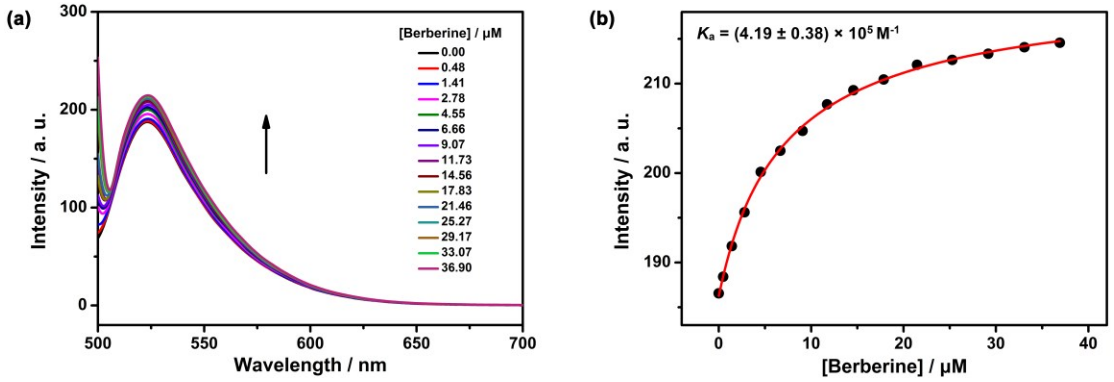

Fig. S14. (a) Competitive fluorescence titration of berberine in the presence of AO/STP3 (1.0/1.0 μM) in HCl solution (pH = 1.2), λ_{ex} = 492 nm. (b) The associated titration curve at λ_{em} = 523 nm and fit according a 1:1 competitive binding model. Data are from n =3 independent experiments and are presented as mean ± SD.

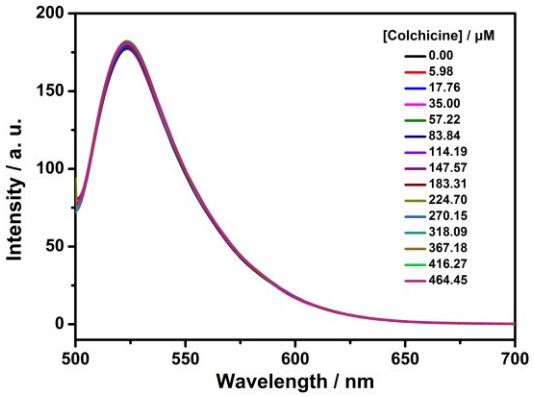

Fig. S15. Competitive fluorescence titration of colchicine in the presence of AO/STP3 (1.0/1.0 μM) in HCl solution (pH = 1.2), λ_{ex} = 492 nm. The recovery of fluorescence is too small relative to the range of quenching, so no reasonable association constant can be obtain.

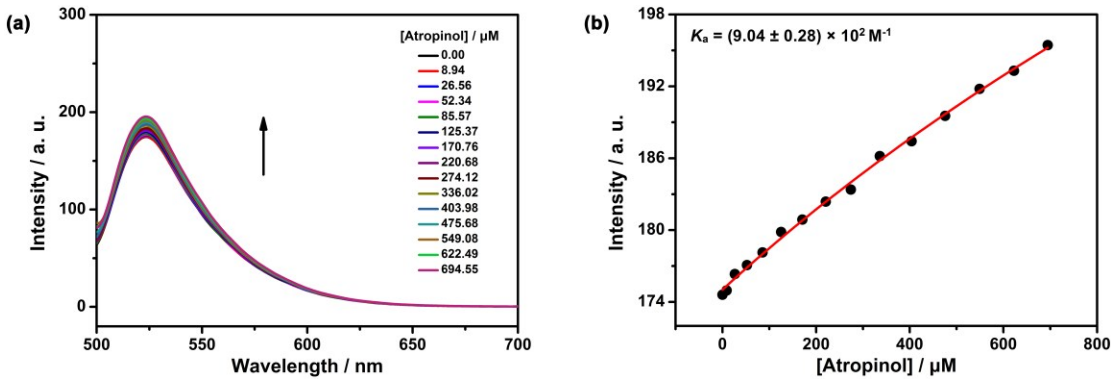

Fig. S16. (a) Competitive fluorescence titration of atropinol in the presence of AO/STP3 (1.0/1.0 μM) in HCl solution (pH = 1.2), λ_{ex} = 492 nm. (b) The associated titration curve at λ_{em} = 523 nm and fit according a 1:1 competitive binding model. Data are from n =3 independent experiments and are presented as mean ± SD.

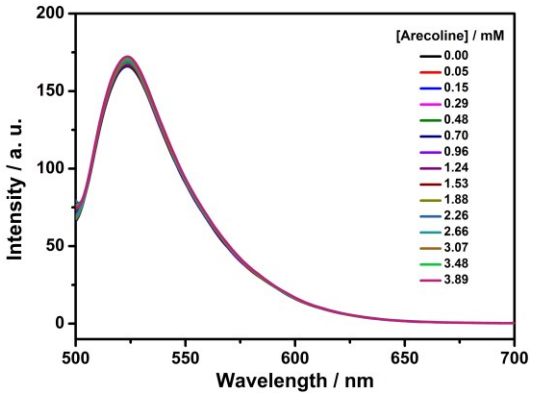

Fig. S17. Competitive fluorescence titration of arecoline in the presence of AO/STP3 (1.0/1.0 μM) in HCl solution (pH = 1.2), λ_{ex} = 492 nm. The recovery of fluorescence is too small relative to the range of quenching, so no reasonable association constant can be obtain.

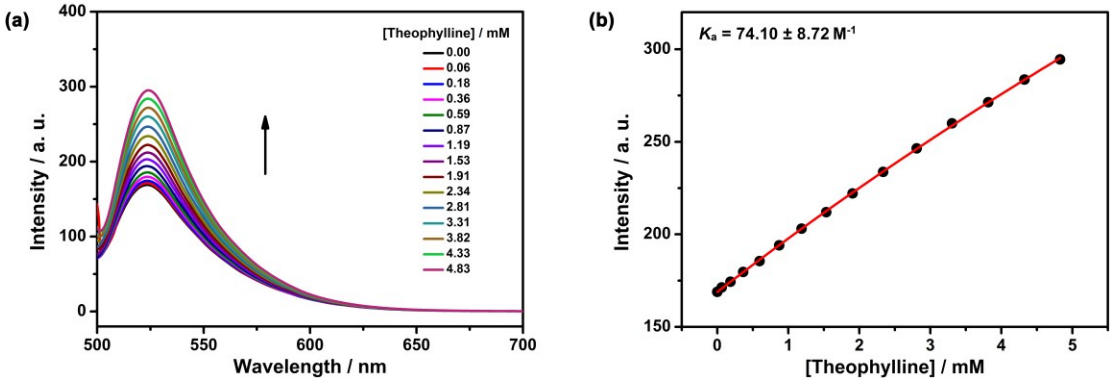

Fig. S18. (a) Competitive fluorescence titration of theophylline in the presence of AO/STP3 (1.0/1.0 μM) in HCl solution (pH = 1.2), λ_{ex} = 492 nm. (b) The associated titration curve at λ_{em} = 523 nm and fit according a 1:1 competitive binding model. Data are from n =3 independent experiments and are presented as mean ± SD.

3.4 Kinetic release profile of alkaloid

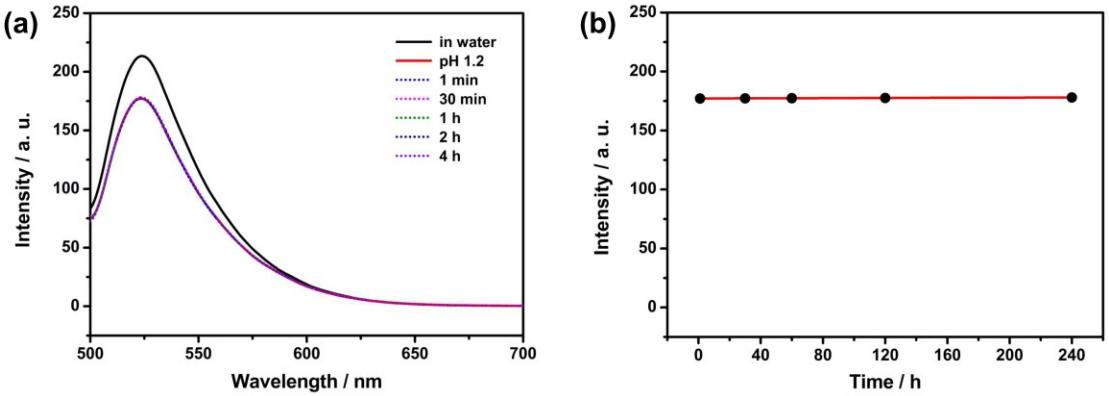

Fig. S19. (a) Fluorescence spectra of AO (1 μM) in the presence of STP3 (1 μM) and colchicine (5 μM) in water and upon adjusting pH to 1.2. (b) The time-dependent change of fluorescence intensity ascribed to AO in sample solution.

3.5 Optimized geometries of various alkaloids with STP3.

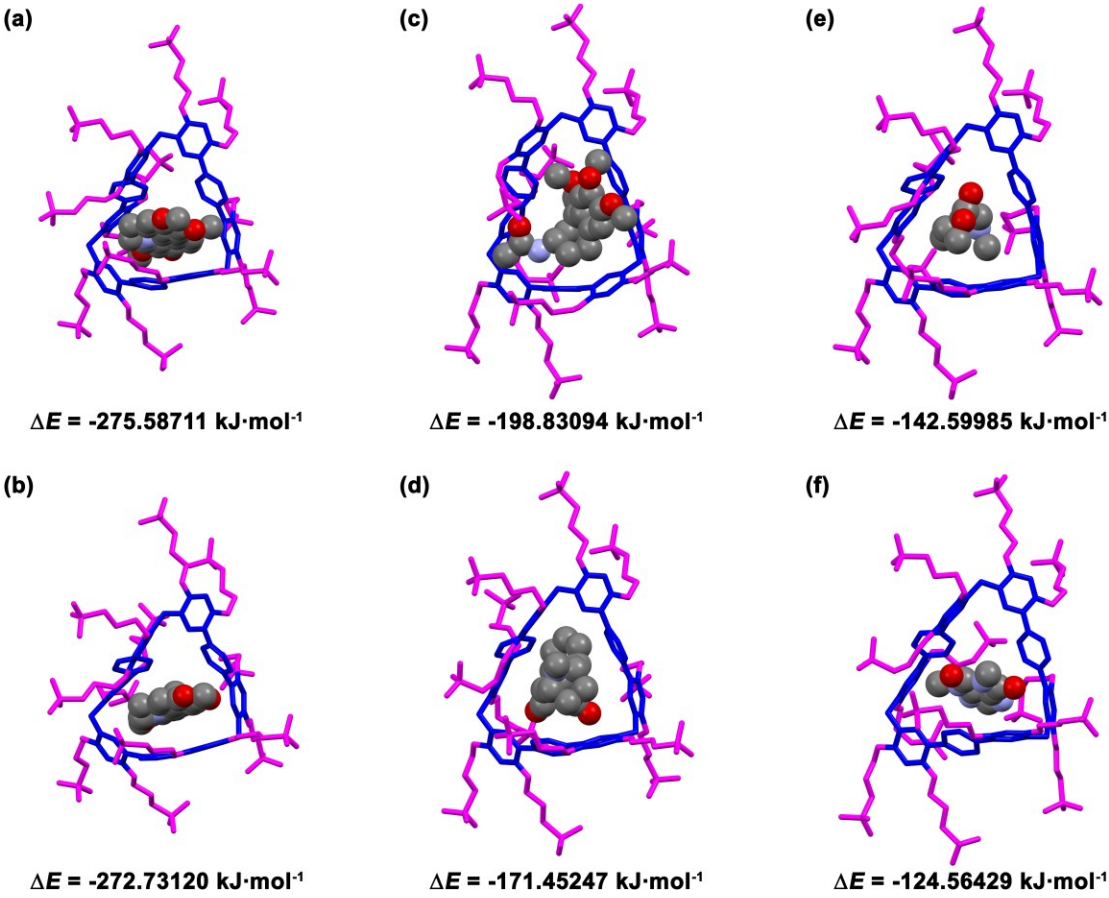

Fig. S20. Optimized geometries, binding energies and structural presentation of (a) palmatine/STP3, (b) berberine/STP3, (c) colchicine/STP3, (d) atropinol/STP3, (e) arecoline/STP3 and (f) theophylline/STP3 complexes in aqueous solution.

3.6 *In vitro* cytotoxicity assay of STP3.

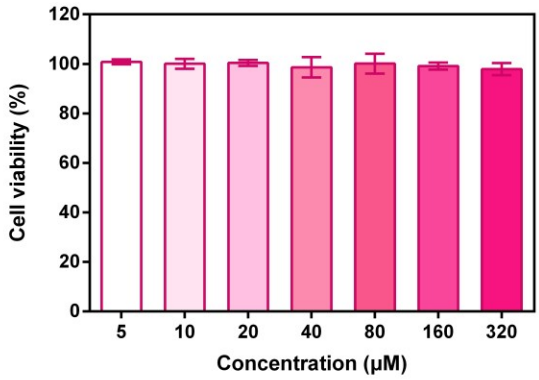

Fig. S21. Relative cell viabilities of GES-1 cells after incubation for 24 h with STP3 at the indicated concentrations measured by CCK-8 assay (mean ± SD, n = 5).

3.7 Body weight change of mice after exposure to STP3.

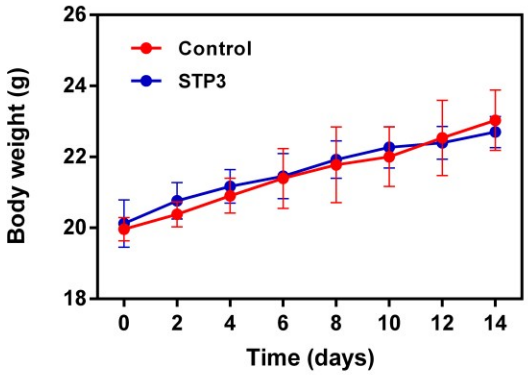

Fig. S22. Change in body weight of mice after exposure to STP3 (50 μM, two-day administration in a row) compared with the control (distilled water) group. Data were represented as mean ± SD, n = 6. This was no statistically significant difference in body change between STP3 and control groups over a period of 14 days.

3.8 Histological H&E staining for stomach, intestine and major oragans.

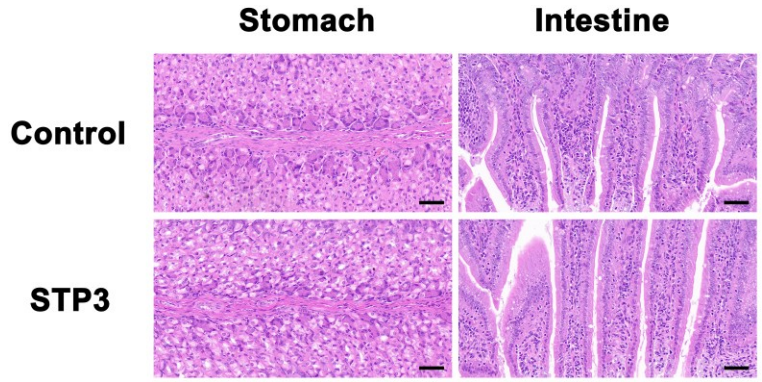

Fig. S23. Histopathologic analysis of stomach and intestine tissue stained with H&E after exposure to distilled water (control) and STP3 (scale bar: 50 μm).

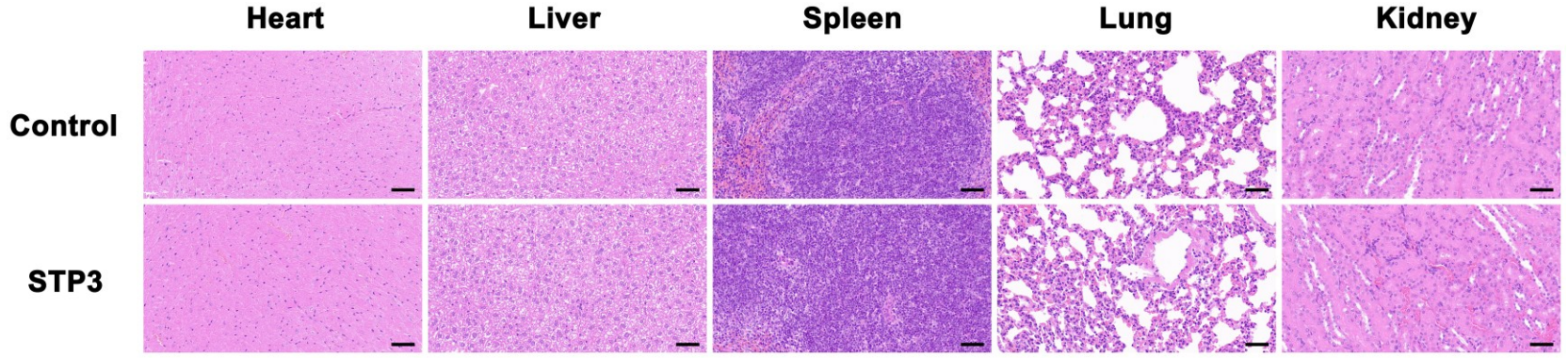

Fig. S24. H&E stains of the major organs from mice after exposure to STP3 compared with the control (distilled water) group (scale bar: 50 μm).

3.9 Determination of antibacterial activity.

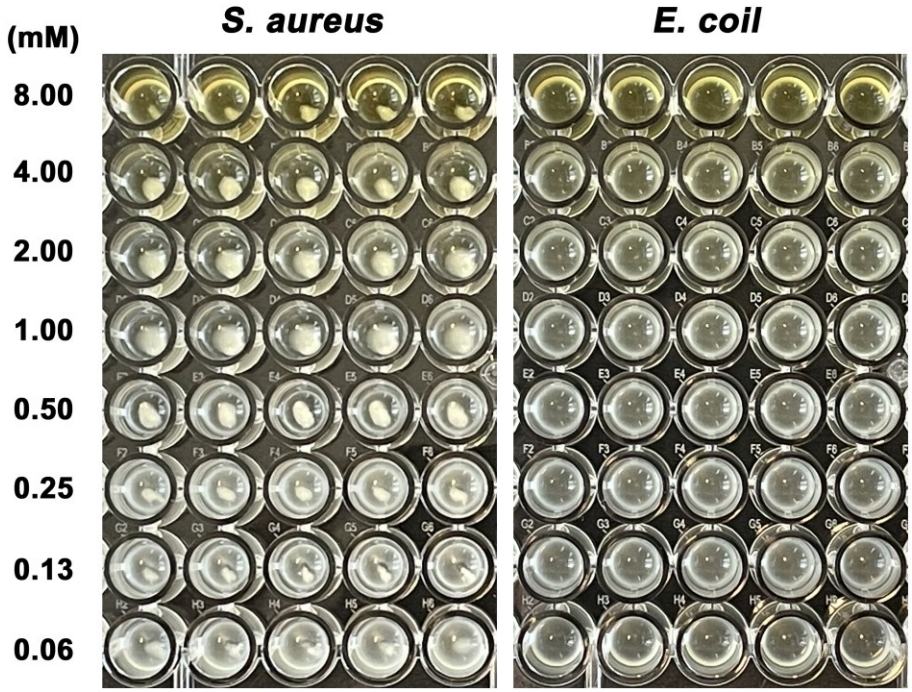

Fig. S25. Antibacterial assay by increasing STP3 concentration against *S. aureus* and *E. coli*. Each concentration of compound was tested in five wells.

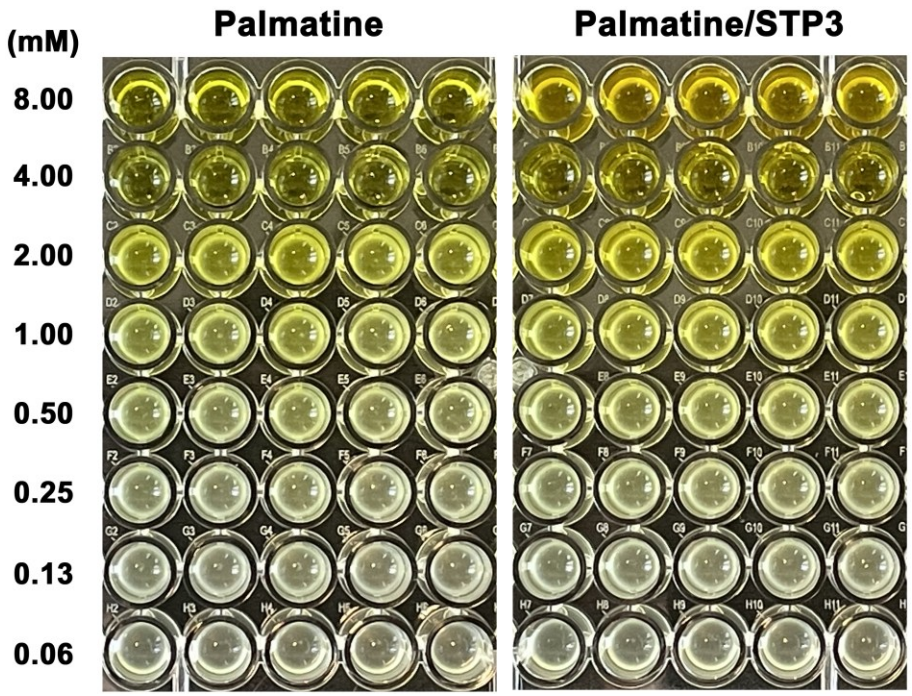

Fig. S26. Antibacterial assay by increasing concentration of palmatine and palmatine/STP3 against *E. coli*. Each concentration of compound was tested in five wells.

References

1. (a) A. Henning, H. Bakirci, W. M. Nau, *Nat. Methods*, 2007, **4**, 629-632. (b) G. Ghale, W. M. Nau, *Acc. Chem. Res.*, 2014, **47**, 947-955. (c) R. N. Dsouza, U. Pischel, W. M. Nau, *Chem. Rev*., 2011, **111**, 7941-7980.

2. J.-Y. Chen, Y.-D. Zhang, Y. Chai, Z. Meng, Y.-H Zhang, L.-M. Chen, D.-Q. Quan, Y.-A. Wang, Q.-B. Meng, C.-J. Li, *Chem. Sci.*, 2021, **12**, 5202-5208.

3. X. Yang, S.-K. Li, Q.-W. Zhang, Y. Zheng, D. Bardelang, L.-H. Wang, R.-B. Wang, *Nanoscale*, 2017, **9**, 10606-10609.

4. J.-Y. Chen, Q.-B. Meng, Y.-D. Zhang, M. Dong, L. Zhao, Y.-H. Zhang, L.-M. Chen, Y. Chai, Z. Meng, C.-H. Wang, X.-S. Jia, C.-J. Li, *Angew. Chem. Int. Ed.*, 2021, **60**, 11288-11293.

5. K.-D. Xu, Z.-Y. Zhang, C.-M. Yu, B. Wang, M. Dong, X.-Q. Zeng, R. Gou, L. Cui, C.-J. Li, *Angew. Chem. Int. Ed.*, 2020, **59**, 7214-7218.